Water-Free Proton-Conducting Polysiloxanes: A Study on the Effect of Heterocycle Structure

Sergio Granados-Focil,† Richard C. Woudenberg,† Ozgur Yavuzcetin,‡ Mark T. Tuominen,‡ and E. Bryan Coughlin*,†

Polymer Science and Engineering Department and Physics Department, University of Massachusetts, Amherst, Massachusetts 01003

Received July 31, 2007; Revised Manuscript Received September 4, 2007

ABSTRACT: Proton-conducting, thermally and electrochemically stable, heterocycle-grafted polysiloxanes have been synthesized via hydrosilylation of vinyl or allyl functionalized weakly basic heterocyclic motifs with a polymethylhydrosiloxane precursor. The basicity of the amphoteric heterocycles was tuned by introducing electron-withdrawing groups, whose presence also produced a decrease in the polymers' glass transition temperature. The proton conductivity depended strongly on the T_g of the polymer matrix and the volume fraction of proton carriers, while the effect of reducing the pK_a of the heterocycle was less pronounced. The resulting polymers showed the highest reported proton conductivities of up to 0.1 mS/cm at temperatures below 80 °C and up to 5 mS/cm at 180 °C when doped with trifluoroacetic acid.

Introduction

The increasing demand for clean, efficient and portable energy devices has motivated the search for new materials to develop environmentally friendly energy utilization.[1−3] An attractive approach consists in the use of polymer electrolyte membrane fuel cells (PEMFC's), due to their high power density and pollution-free fuel consumption.[3,4] An obstacle for commercialization of PEMFCs is the lack of better performing, more cost-effective materials.[4−6] The majority of the systems currently under evaluation rely on water as the conduction medium, which restricts their use temperature to ∼100 °C.[5−7] However, development of PEMFCs capable of operating at temperatures close to 200 °C would result in several key improvements that are essential for the widespread use of fuel cells in everyday applications. Systems operating at elevated temperatures are more efficient, reduce the cell cost by decreasing the required platinum loading, and simplify the overall heat management of the device.[8]

Kreuer and co-workers[9,10] proposed an attractive alternative approach where amphoteric heterocycles were used as the proton-conducting species. Proton transport within heterocyclic hydrogen-bonded networks occurs under both anhydrous and low relative humidity conditions and could thus be used to develop polymer membranes that are highly conductive at temperatures above the boiling point of water. These materials would enable PEMFCs to function without the need of external humidification and at temperatures well above 100 °C. Previous work using imidazole and benzimidazole as the proton-conducting motifs suggests that proton conductivity depends on the local mobility of the heterocycles within the polymer films and on the effective concentration of mobile protons in the membranes.[11−16] The proton conductivity of these systems increased when varying amounts of strong acids were added; such an increase was attributed to a higher concentration of mobile protons due to protonation of some of the heterocycles within the polymer matrix.[14] A pronounced relative increase in proton conductivity was reported by Liu and co-workers when they compared vinyl heterocycle polymers where the imidazole pendant groups had been substituted by 1,2,3-triazole.[17] The higher conductivity was ascribed to a reduction in the heterocycle pK_a and to a smaller number of conformational changes needed for conduction when triazoles are compared to imidazoles.[18] Further support for this hypothesis was provided through a model compound study by Subbaraman et al.[19] describing the influence of proton affinity (pK_a) in facilitating proton transport within amphoteric heterocyclic systems. Although both studies strongly suggested advantages when using lower pK_a heterocyclic motifs, efforts aimed at decoupling the effects of heterocycle pK_a from its chemical structure have not been reported. Furthermore, the effect of heterocycle structure on the properties of the resulting polymer matrices remains an open question. Previous work in our group has systematically studied the effect of polymer backbone mobility,[20] and heterocycle nature,[21] on proton conductivity.

Prompted by all of these previous reports, we have now developed highly mobile polymer matrices containing weakly basic heterocyclic motifs designed to better gauge the contributions of both chemical structure and pK_a on the conductivity and properties of the resulting polymers We report the synthesis and properties of chemically and electrochemically robust polysiloxanes containing pendant 1,2,3-triazole (pK_a = 9)[22] and 2-trifluoromethylbenzimidazole (pK_a = 8)[23] as the proton-conducting groups. The present study revealed that the heterocycle pK_a has little effect on the conductivity of the resulting polymers, while the proton carrier mass fraction within the polymer matrix, as well as the T_g of polymer backbone, play a much more significant role. The combination of flexible polymeric backbones and readily accessible acid-doped 1,2,3-triazoles produced materials exhibiting water-free proton conductivities higher than those previously reported at temperatures below 100 °C.

Experimental Section

Materials. Azidomethyl pivalate was prepared as reported in the literature.[24] All other reagents were purchased from Sigma-Aldrich and used as received. THF and toluene were distilled over

* Corresponding author. E-mail: Coughlin@mail.pse.umass.edu.
† Polymer Science and Engineering Department.
‡ Physics Department.

10.1021/ma071715q CCC: $37.00
Published on Web 11/01/2007

sodium/benzophenone prior to use. DMF was distilled over calcium hydride prior to use.

Synthesis of 6-Allyloxyhex-1-yne (1). To a clean, dry, nitrogen-purged 250 mL two-neck round-bottom flask were added sodium hydride (1.44 g, 0.06 mol) and anhydrous DMF (45 mL). The slurry was cooled to 0 °C followed by dropwise addition of 5-hexyn-1-ol (3.37 mL, 0.03 mol) under constant agitation. The mixture was stirred for 30 min and allowed to come to room temperature. Allyl bromide (2.46 mL, 0.028 mol) was added dropwise under constant agitation, and the mixture was allowed to stir for 2 h at room temperature. The reaction was ended by addition of a large excess of water (200 mL) and the product extracted with dichloromethane (5 × 25 mL). The combined organic layers were dried over anhydrous $MgSO_4$ and filtered; solvent was removed under reduced pressure to yield 6-allyloxyhex-1-yne (**1**) as a pale yellow liquid (3.35 g, 86.8%) which was used without further purification. ^{1}H NMR ($CDCl_3$): δ 1.79 (4H, m), 1.95 (1H, t), 2.22 (2H, m), 3.47 (2H, t), 3.96 (2H, d), 5.18 (1H, dd), 5.25 (1H, dd), 5.89 (1H, m). ^{13}C NMR ($CDCl_3$): δ 18.23, 25.23, 28.76, 68.42, 69.71, 71.81, 84.33, 116.78, 134.96. Mass spectrum *m*/*z* 137.09 (10, $M^{\bullet+}$), 123.08 (10), 109.05 (17), 97.06 (25), 79.03 (100), 67.06 (40), 53.12 (57).

Synthesis of But-3-en-1-ynyltrimethylsilane (2). Compound **2** was prepared following a procedure reported previously[25] and obtained as clear liquid in 68% yield. ^{1}H NMR ($CDCl_3$): δ 5.83 (1H, dd), 5.71 (1H, dd), 5.50 (1H, dd), 0.201(9H, s). ^{13}C NMR ($CDCl_3$): δ −1.43, 95.55, 102.95, 116.17, 128.60.

Synthesis of 2,2-Dimethylpropionic Acid 4-Vinyl-4,5-dihydro-[1,2,3]triazol-1-ylmethyl Ester (3). 1 g (8 mmol) of **2**, 0.4 g (1.6 mmol) of $CuSO_4 \cdot 5H_2O$, 0.32 g (1.6 mmol) of sodium ascorbate, 20 mL of a 1:1 mixture of *t*-BuOH and H_2O, and 1.6 mL of 1.0 M solution of Bu_4NF in THF were added to a 50 mL round-bottom flask equipped with a magnetic stirrer. The mixture was stirred at room temperature for 24 h and the resulting greenish solution was diluted with water (50 mL) and extracted with ethyl acetate (3 × 25 mL). The combined organic layer was first washed with 5% NH_4OH (3 × 100 mL) and then with brine (100 mL) and finally dried over magnesium sulfate. The excess solvent was removed via rotary evaporation to yield 1.4 g (7.1 mmol, 88%) of **3**. ^{1}H NMR ($CDCl_3$): δ 7.75 (1H, s), 6.71 (1H, dd), 6.22 (2H, s), 5.97 (1H, d), 5.39 (1H), 1.2 (9H). ^{13}C NMR ($CDCl_3$): δ 178.38, 147.09, 125.77, 122.24, 117.65, 70.38, 39.12, 25.58.

Synthesis of 2,2-Dimethylpropionic Acid 4-(4-Allyloxybutyl)-[1,2,3]triazol-1-ylmethyl Ester (4). To 4 g (29 mmol) of **1** were added a mixture of *t*-BuOH/water (2/1) (93 mL) and $CuSO_4 \cdot 5H_2O$ (1.5 mL of a 1.0 M solution, 1.5 mmol) followed by a 1.0 M solution of sodium ascorbate (3.0 mL, 3.0 mmol) and azidomethyl pivalate (6.12 g, 0.039 mol). The mixture was stirred vigorously for 18 h at room temperature. The reaction was diluted with water and the product extracted with ethyl acetate (2 × 100 mL). The combined organic layers were washed with 5% NH_4OH (2 × 100 mL) and brine, dried over $MgSO_4$, and filtered, and solvent was removed under reduced pressure. Purification was performed by flash chromatography (ethyl acetate/hexanes 1:1) to yield 2,2-dimethylpropionic acid 4-(4-allyloxybutyl)[1,2,3]triazol-1-ylmethyl ester as a clear liquid (7.04 g, 84%). ^{1}H NMR ($CDCl_3$): δ 1.64 (2H, quin), 1.73 (2H, quin), 2.75 (2H, t), 3.45 (2H, t), 3.94 (2H, d), 5.14 (1H, d), 5.23 (1H, d), 5.89 (1H, m), 6.19 (2H, s), 7.53 (1H, s). ^{13}C NMR ($CDCl_3$): δ 25.06, 25.68, 26.58, 28.98, 38.54, 69.39, 69.67, 71.57, 116.57, 121.91, 134.68, 148.39, 177.56. Mass spectrum *m*/*z* 295.2 (20, $M^{\bullet+}$), 254.2 (40), 238.2 (20), 210.1 (20), 197.1 (15), 180.1 (15), 140.1 (40), 124.1 (100), 81.0 (70), 57.1 (50).

Synthesis of Bromo-2-trifluoromethyl-1-(2-trimethylsilanylethoxymethyl)-1*H*-benzimidazole (5). 10 g (53.46 mmol) of 4-bromobenzene-1,2-diamine, 100 mL of 4 M aqueous HCl, and 5 mL of trifluoroacetic acid (64.9 mmol) were added to a 250 mL round-bottom flask fitted with a condenser and a magnetic stirrer. The resulting suspension was heated to reflux and stirred for 4 h. Then the reaction mixture was allowed to cool to room temperature and the resulting solid filtered. The crude dark red product was dissolved in 200 mL of methanol and refluxed for 30 min in the presence of 3 g of activated charcoal; the resulting light orange solution was filtered to separate the solids and concentrated to 75 mL. For the final recrystallization step, the methanol solution was diluted with 25 mL of water and allowed to cool to room temperature to yield 12.18 g (46 mmol, 86% yield) of 5-bromo-2-trifluoromethylbenzimidazole, BrBzTF, as off-white crystals. BrBzTF was dried at 50 °C under vacuum for 6 h before being used in the next synthesis step. 5 g (18.85 mmol) of BrBzTF was dissolved in 25 mL of dry DMF and added slowly to an ice-cooled suspension of 37.77 mmol (1.5 g of 60% mineral oil suspension) of NaH in 50 mL of dry DMF. After addition of the BrBzTF solution, 3.33 mL (18.95 mmol) of 2-(chloromethoxy)ethyltrimethylsilane (SEM-Cl) were added to the reaction mixture which was then allowed to warm to room temperature and stirred for 5 h. The resulting suspension was poured in to 300 g of crushed ice and stirred for 20 min. The crude product, 6.96 g (17.63 mmol, 93% yield), a mixture of the two tautomers (60:40) 5-bromo-2-trifluoromethyl-1-(2-trimethylsilanylethoxymethyl)-1*H*-benzimidazole **(5)** and 6-bromo-2-trifluoromethyl-1-(2-trimethylsilanylethoxymethyl)-1*H*-benzimidazole, was dried under vacuum at 40 °C for 12 h and used without further purification. ^{1}H NMR (DMSO-d_6): δ 8.25 (0.4H, d), 8.14 (0.6H,d), 7.93 (0.6H, d), 7.85 (0.4H, d), 7.70 (0.6H, dd), 7.59 (0.4H,dd), 5.80 (2H, s), 3.56 (2H, m), 0.84 (2H, m), 0.084 (9H, s). ^{13}C NMR ($CDCl_3$): δ 146.32, 141.4 (q), 134.33, 129.03, 128.21, 127.73, 124.39, 121.5 (q), 119.36, 117.16, 114.83, 112.94, 74.17, 67.09, 17.70, −1.53. Mass spectrum *m*/*z* 394 ($M^{\bullet+}$ − 1), 396 ($M^{\bullet+}$ + 1).

Synthesis of 5-Vinyl-2-trifluoromethyl-1-(2-trimethylsilanylethoxymethyl)-1*H*-benzimidazole (6). In a drybox, 50 mL of toluene, 5 g (12.26 mmol) of **5**, 112 mg (0.126 mmol) of $Pd_2(dba)_3$, and 3 mL of a 0.1 M solution (0.277 mmol) of tri-*tert*-butylphosphine were added to a round-bottom flask fitted with a magnetic stirring bar. After a homogeneous solution was formed, 3.7 mL (12.6 mmol) of vinyltributyltin was added, and the reaction mixture was stirred at room temperature for 36 h. The reaction was stopped by addition of 50 mL of diethyl ether and 2 g of finely ground potassium fluoride. After stirring the resulting suspension, the solids were separated by filtration and the resulting solution was passed through a mixture of 5 g of finely powdered potassium fluoride and 50 g of silica gel. Finally, the product was isolated by column chromatography (4:1 hexanes:ethyl acetate) to yield 3.32 g (9.7 mmol, 77% yield) of **6** as the mixture of tautomers (approximately 60:40). ^{1}H NMR ($CDCl_3$): δ 7.87 (0.4H, d), 7.82 (0.6H, d), 7.59 (1.4H, m), 7.52 (0.6H, dd), 6.86 (1H, dd), 5.85 (0.54H, dd), 5.78 (0.46H, dd), 5.67 (2H, d), 5.34 (0.58H, dd), 5.29 (0.40H, dd), 3.57 (2H, m), 0.93 (2H, m), 0.043 (9H, s). ^{13}C NMR ($CDCl_3$): δ 140.96, 136.66 (q), 135.81, 122.59, 121.5 (q), 121.49, 114.73, 109.29, 119.36, 117.16, 114.83, 112.94, 73.92, 66.94, 17.71, −1.50. Mass spectrum *m*/*z* 342 ($M^{\bullet+}$).

Synthesis of Tz2Si (7). In a drybox, 1 g (5 mmol) of **3**, 200 mg (3.3 mmol) of PHMS, and 5 mL of dry toluene were added to a glass vial equipped with a magnetic stirrer and a rubber septum. The mixture was stirred for 5 min, and then 5 drops of Karstedt's catalyst were added; the solution changed from colorless to light yellow. After addition of the catalyst, the vial was removed from the drybox and stirred at 75 °C for 48 h. The reaction was then diluted with diethyl ether (10 mL) and filtered through a silica pad followed by extensive washing with ether (100 mL). The excess solvent was removed by rotary evaporation and purification was accomplished by column chromatography. A mixture of ethyl acetate:hexanes (1:1) was used to remove the unreacted vinyltriazole (**3**); the POM-Tz2Si polymer was removed from the column by elution with ethyl acetate:methanol 5:1. The pivaloyl protecting group was removed by treatment with sodium methoxide. To a clean, dry, 100 mL round-bottom flask equipped with a stir bar was added triazole-POM functionalized polysiloxane (500 mg, 1.94 mequiv) and ethylenediamine (235 μL, 7.05 mequiv). Under constant agitation, 0.1 M NaOH/MeOH (31 mL, 3.1 mequiv) was added to the flask. The reaction mixture was stirred for 90 min

and then poured slowly into pH 7 buffer solution. The buffer pH was monitored and kept from exceeding pH 8 by adding 1.0 M HCl as necessary. Final pH was adjusted to 8 followed by extraction with ethyl acetate:dichloromethane (1:1) (5 × 30 mL) to remove the polymer (triazole-2-siloxane, Tz2Si, **7**). Solvent was removed under reduced pressure to yield an opaque viscous oil (214 mg, 77%). ^{1}H NMR (DMSO-d_6): δ 0.041 (3H, s), 0.88 (1.5H, m), 1.28 (1.5H, m), 2.28 (0.5H, m), 2.65 (0.5, m), 7.44 (1H, m), 14.57 (1H, s) ^{13}C NMR (DMSO-d_6): δ −3.04, −1.22, 13.13, 15.90, 17.64, 19.07, 130.74, 148.41.

Synthesis of Tz8Si (8). Polysiloxane **8** was prepared via the same procedure described for **7** using **4** (698 mg, 2.5 mequiv) and poly(methylhydrosiloxane) (100 mg, 1.67 mequiv) as starting materials to yield an opaque viscous oil (303 mg, 72%). ^{1}H NMR (DMSO-d_6): δ 0.044 (3H, s), 0.48 (2H, m), 1.50 (4H, m), 1.60 (2H, quin), 2.64 (2H, t), 3.29 (4H, t), 7.54 (1H, s), 14.6 (1H, s). ^{13}C NMR (DMSO-d_6): δ −0.79, 12.68, 22.70, 24.48, 25.60, 28.74, 69.43, 72.14, 131.71, 146.35.

Synthesis of FBz2Si (9). Polysiloxane **9** was prepared via the same hydrosilylation procedure described for **7** using **6** (1.15 g, 3.36 mmol) and poly(methylhydrosiloxane) (150 mg, 2.5 mequiv) as the starting materials to yield the SEM-protected intermediate as a viscous clear oil (685 mg, 69% yield). The SEM protecting group was cleaved using HCl/MeOH as follows: to a clean, dry, 25 mL round-bottom flask equipped with stir bar were added 2-trifluoromethyl-SEM protected benzimidazole functionalized siloxane polymer (500 mg, 1.23 mequiv) and 10 mL of methanol. Under constant agitation, 3 mL of 5 M HCl/MeOH were added to the flask. The reaction mixture was stirred overnight; then the excess methanol was evaporated and the residue poured into water. The resulting solid polysiloxane was filtered, redissolved in methanol, and precipitated into a pH 8 sodium bicarbonate solution. The polymer was filtered and dried under vacuum to yield 285 mg (85%) of **9**. ^{1}H NMR (DMSO-d_6): δ 0.03 (3H, s), 0.86 (1H, m), 1.27 (1.5H, m), 2.03 (0.5H, m), 2.72 (1H, m), 7.43 (3H, m), 7.54 (1H, s), 13.67 (1H, bs). ^{13}C NMR (DMSO-d_6): δ −2.34, −0.49, 5.54, 15.1, 19.64, 29.05, 118.21, 120.89, 124.66, 125.63, 134.67, 140.31.

Synthesis of Polyvinyltriazole (PVT). 500 mg of **3** and 15 mg of AIBN were dissolved in 5 mL of THF, and the resulting solution was subjected to two freeze−pump−thaw cycles before heating to 70 °C for 6 h. The resulting POM protected polyvinyltriazole (460 mg, 92% yield), M_n = 21 000, PDI 2.5, was precipitated in hexane and dried under vacuum prior to deprotection using the same protocol described for **7** to yield 190 mg (78.8% yield) of polyvinyltriazole (PVT). ^{1}H NMR (DMSO-d_6): δ 13.96 (1H, s), 7.15 (1H, bs), 2.08 (1H, bs), 1.56 (2H, bs). ^{13}C NMR (DMSO-d_6): δ 147.25, 128.71, 36.95, 31.29.

Characterization. ^{1}H NMR (300 MHz) and ^{13}C NMR (75 MHz) spectra were obtained on a Bruker DPX-300 NMR spectrometer with the samples dissolved in either chloroform-*d* or dimethyl-d_6 sulfoxide (DMSO-d_6). Thermogravimetric analysis (TGA) was carried out using a TA Instruments TGA 2950 thermogravimetric analyzer with a heating rate of 10 °C/min from room temperature to 600 °C under nitrogen purge. Glass transition temperatures were obtained by differential scanning calorimetry (DSC) using a TA Instruments Dupont DSC 2910. Samples of approximately 3−5 mg were used, with a heating rate of 10 °C/min from −100 to 180 °C under a flow of nitrogen (50 mL/min), and the midpoint of the observed step transition was taken as T_g. Electrochemical impedance data were obtained using a Solartron 1287 potentiostat/1252A frequency response analyzer in the 0.1 Hz−300 kHz range. The polymers were dried under vacuum at 50 °C overnight before being pressed between two gold-coated blocking electrodes followed by an application of 100 mV excitation voltage with a logarithmic frequency sweep from 3 × 10^5 to 1 × 10^{-1} Hz. The sample thickness and contact surface area were controlled by using a 125 μm thick Kapton tape spacer. Resistance values were taken at the minimum imaginary response in a Z' vs Z'' plot. The measurements were performed under vacuum to ensure an anhydrous environment.

Scheme 1. Synthesis of 2,2-Dimethylpropionic Acid 5-Vinyl-[1,2,3]triazol-1-ylmethyl Ester (3), 2,2-Dimethylpropionic Acid 4-(4-Allyloxybutyl)[1,2,3]triazol-1-ymethyl Ester (4), and 4-Vinyl-2-trifluoromethylbenzimidazole (6)[a]

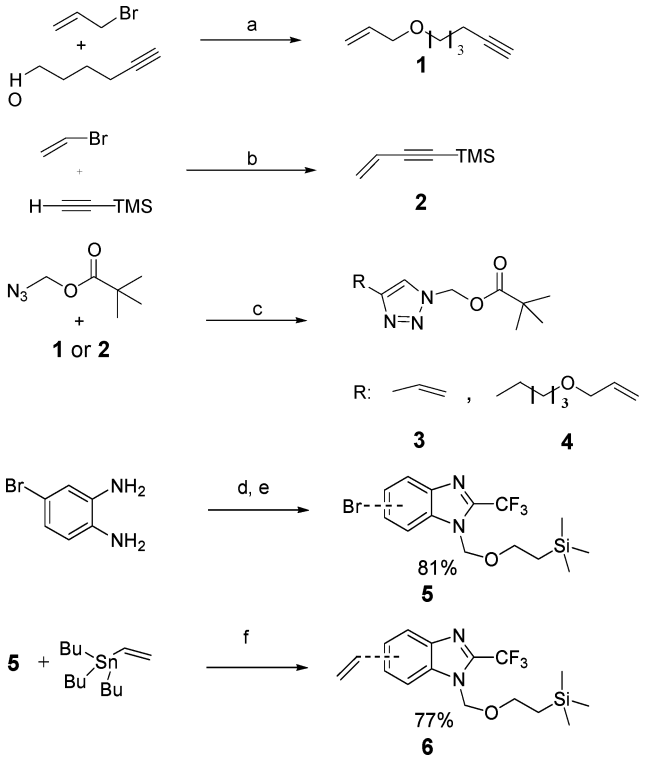

[a] a: NaH/DMF, RT, 2 h. b: $PdCl_2(PPh_3)_2$, CuI, Et_3N, 36 h. c: $CuSO_4$, sodium ascorbate, tBuOH/H_2O (2:1), and Bu_4NF (1.1 equiv only for the synthesis of **3**), 18 h. d: trifluoroacetic acid (2 equiv), 4.0 M aq HCl. e: 2-(chloromethoxy)ethyltrimethylsilane (SEM-Cl), NaH/DMF, RT, 3 h. f: $(Pd)_2(dba)_3$, tri-*tert*-butylphosphine, toluene, RT, 12 h.

Scheme 2. Synthesis of Heterocycle-Grafted Polysiloxanes[a]

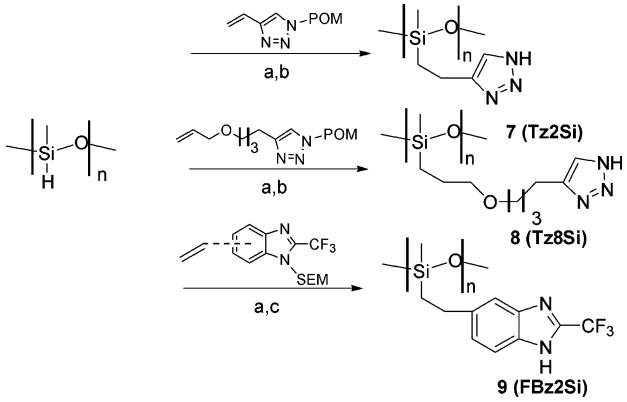

[a] a: Toluene, Pt^0, 50 °C, 36 h. b: 0.1 M NaOH/MeOH and triethylamine for 1.5 h. c: 1.0 M HCl/MeOH.

Results and Discussion

Synthesis. Facile access to the precursor vinyl- or allyl-functionalized heterocyclic compounds was achieved by combining and adapting several procedures to develop the synthetic routes illustrated in Scheme 1.[23−26] Compounds **3**, **4**, and **6** were attached to the siloxane backbone via Pt^0-catalyzed hydrosilylation of the vinyl-functionalized heterocycles with a polymethylhydrosiloxane (2000 g/mol) precursor (see Scheme 2).

Thermal Analysis. TGA and DSC analysis results are summarized in Table 1. The polysiloxanes are thermally stable

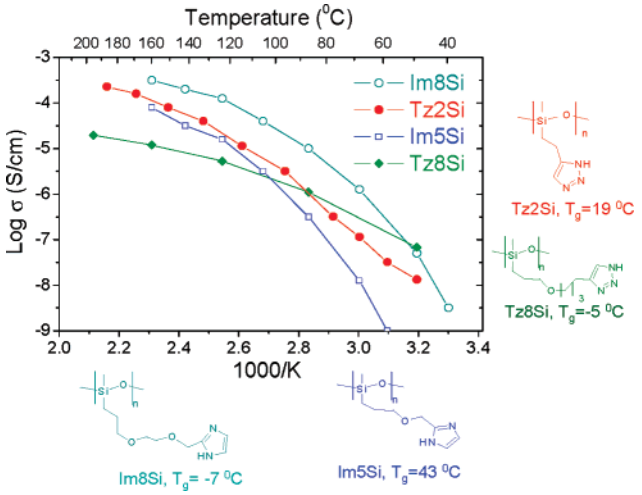

Figure 1. Proton conductivity vs 1000/K for polymers Tz2Si and Tz8Si, along with Im5Si and Im8Si for comparison.[27]

Table 1. Glass Transition Temperatures and Decomposition Onset Temperatures for Heterocycle-Containing Polysiloxanes

material	glass transition (°C)	decompn onset (2% weight loss (°C))
Tz2Si	19	180
Tz2Si, 25% TFA	24	178
Tz2Si, 75% TFA	21	175
Tz2Si, 100% TFA	22	183
Tz8Si	−5	252
Tz8Si, 25% TFA	−15	202
Tz8Si, 50% TFA	−12	157
Tz8Si, 75% TFA	NA	NA
Tz8Si, 100% TFA	−11	154
FBz2Si	5	211
FBz2Si 5% TFA	8	205
FBz2Si 10% TFA	10	201
FBz2Si 15% TFA	11	203
polyvinyltriazole	48	164

up to 180 °C under nitrogen. Slow heating (1 °C/min) of these materials under air showed a 10% weight loss at 175 °C, suggesting that the chemical structure may require further optimization before being used for membrane electrode assemblies. However, the materials are stable to the conditions used during impedance measurements. Furthermore, thermal cycling of the polymer samples inside the vacuum oven did not produce appreciable changes in the electrical impedance or the chemical structure. The glass transition temperature of the 1,2,3-triazole-containing polysiloxanes decreases as the alkyl chain spacer length increases; **7 (**Tz2Si**)** and **8 (**Tz8Si**)** have a T_g of 19 and −5 °C, respectively. The increase in the spacer length from two to eight atoms between the polymer backbone and the heterocycle resulted in a 25 °C decrease in glass transition temperature. The 2-trifluoromethylbenzimidazole-containing analogue, **9 (**FBz2Si**)**, showed a glass transition at 5 °C.

Proton Conductivity. The polymeric materials Tz8Si and Tz2Si exhibit proton conductivities ranging from $10^{-3.6}$ S/cm at 200 °C to $10^{-7.5}$ S/cm at 40 °C and are compared with imidazole-functionalized polysiloxanes, Im8Si and Im5Si, reported earlier by Meyer in Figure 1.[27] All polymers showed a nonlinear temperature dependence of the conductivity consistent with previous observations linking the proton transport to the mobility of the polymer matrix.[14] The proton conductivity of the compounds presented in Figure 1 depends on several factors, such as heterocycle volume fraction within the polymer matrix,

Table 2. Heterocycle Mass Fractions and T_g for Triazole- and Imidazole-Containing Polysiloxanes

material	glass transition temp (°C)	heterocycle mass fraction (wt %)
Tz2Si	19	43
Tz8Si	−5	28
Im5Si	41	36
Im8Si	7	28

heterocycle structure, and polymer glass transition temperature. Insight into the effect of heterocycle structure on proton conductivity can be obtained by analysis of the curves for Tz8Si and Im8Si. Both polymers have the same heterocycle mass fraction (28%), but the conductivity of Im8Si diverges from that of Tz8Si as the temperature increases. The glass transition temperature of Im8Si is 12 °C higher than that of Tz8Si, suggesting that the imidazole motifs form a less mobile, more tightly bound, hydrogen-bonded network. This accounts for the more pronounced temperature dependence on conductivity of Im8Si compared to Tz8Si. In spite of its higher T_g, Im8Si showed comparable or higher conductivity than Tz8Si, indicating that the heterocycle structure plays a significant role on the conductivity of the resulting polymer. Furthermore, the lower pK_a of the triazole heterocycles does not translate into higher proton conductivities as expected from previous reports.[17,19]

A striking difference between the imidazole- and triazole-containing polysiloxanes is the effect of heterocycle concentration on their proton transport ability. The mass fractions of heterocycle within the polymer matrix for the imidazole- and triazole-containing polysiloxanes are summarized in Table 2.

In the case of the imidazole-containing polysiloxanes, a decrease in heterocycle mass fraction, from Im5Si to Im8Si (Δwt % = −8%), resulted in decreased polymer glass transition temperature ($\Delta T_g = -34$ °C) and increased proton conductivity, while showing essentially the same temperature dependence. In contrast, a larger decrease in the triazole mass fraction from Tz2Si to Tz8Si (Δwt % = −15%) resulted in a less pronounced decrease in polymer glass transition ($\Delta T_g = -24$ °C) but produced a more complex effect in the proton conductivity. Reduced triazole mass fraction lowered the proton conductivity at high temperatures and resulted in a less pronounced temperature dependence. This suggests that Tz8Si has a lower apparent activation energy for proton transport than Tz2Si as a result of improved local mobility; however, the lower conductivity at elevated temperatures indicates that charge carrier density becomes the main limiting factor.

Such disparity in the influence of heterocycle concentration on conductivity suggests that a simple change in chemical structure of the proton-conducting motifs can have a complex effect on the resulting hydrogen-bonded network. Specifically, that the delicate balance between two competing factors affecting proton transport, charge carrier density and polymer matrix mobility, depends critically on the chemical structure of the heterocycle. Imidazole produces hydrogen-bonded networks whose conductivity is less sensitive to changes in heterocycle volume fraction than their 1,2,3-triazole counterparts. Alternatively, the T_g of the imidazole-containing materials is more sensitive to changes in volume fraction than that of the 1,2,3-triazole analogues. Therefore, the optimal charge carrier mass fraction that maximizes proton conductivity will vary depending on the particular heterocycle being utilized.

In order to deconvolute the contribution of polymer glass transition and heterocycle mass fraction to proton conductivity, it is useful to plot the data in Figure 1 as a function of a reference temperature ($T - T_g$) (see Figure 2).

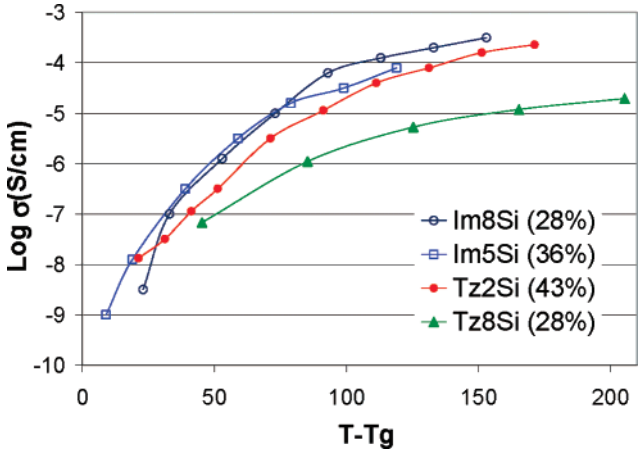

Figure 2. Proton conductivity vs $T - T_g$ for polymers Tz2Si and Tz8Si, along with Im5Si[27] and Im8Si[27] for comparison. The mass fraction of the five-membered heterocyclic ring is included in parentheses for reference.

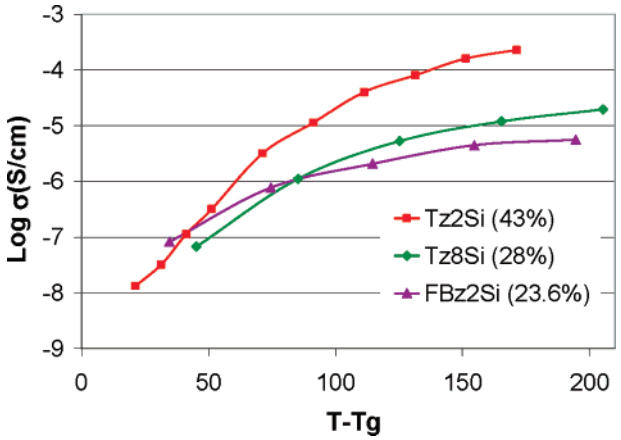

Figure 3. Proton conductivity vs $T - T_g$ for polymers Tz2Si, Tz8Si, and FBz2Si. The mass fraction of the five-membered heterocyclic ring is included in parentheses for reference.

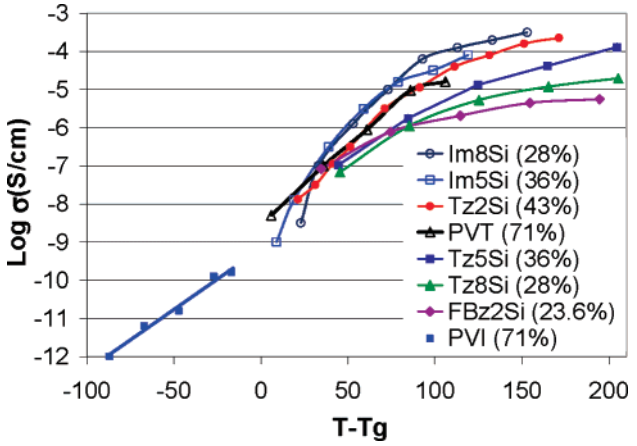

Figure 4. Proton conductivity vs $T - T_g$ for polymers Tz2Si, Tz8Si, and FBz2Si, along with Im5Si,[27] Im8Si,[27] polyvinylimidazole (PVI),[28] and polyvinyltriazole (PVT)[17] for comparison. The mass fraction of the five-membered heterocyclic ring is included in parentheses for reference.

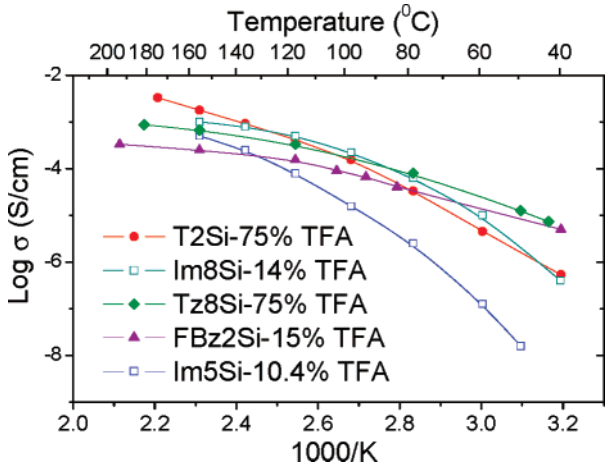

Figure 5. Proton conductivity vs 1000/K for TFA-doped polymers Tz2Si, Tz8Si, and FBz2Si, along with Im5Si and Im8Si for comparison.

At temperatures 50 °C above glass transition temperature, the proton transport is limited by the concentration of proton carriers as indicated by the higher conductivity of Tz2Si compared to that of Tz8Si. On the other hand, at temperatures between T_g and $T_g + 50$ °C, the polymer matrix mobility limits the proton transport as indicated by the convergence of all data into the same "master" trend. A decrease in imidazole mass fraction from 34% in Im5Si to 28% in Im8Si results in an order of magnitude increase in the proton conductivity. However, plotted as a function of the reference temperature ($T - T_g$), the convergence of the two curves indicates that, for these materials, proton transport is mainly limited by T_g and, therefore, polymer backbone mobility. The convergence of Tz2Si with the imidazole materials indicates that once a minimum threshold of charge carrier density is reached, the behavior of tethered imidazole and 1,2,3-triazole materials is nearly identical; this indicates that the pK_a of the heterocycle does not play a significant role in determining proton conductivity. To further explore the effect of heterocycle nature on proton conductivity, another polysiloxane, FBz2Si, containing a bulkier and weakly basic heterocycle, 2-trifluoromethylbenzimidazole, was prepared and compared with the analog Tz2Si and Tz8Si (see Figure 3).

Although the basicity of the heterocyclic motifs in Tz2Si and FBz2Si is comparable, their proton transport ability is not determined by their pK_a but rather by a combination of the polymer matrix T_g and the volume fraction of the heterocyclic ring. Modification of the heterocyclic structure from imidazole to 2-trifluoromethylbenzimidazole had a similar effect as the one observed when "diluting" the heterocycles by increasing the tether chain length from 2 to 8 atoms in Tz2Si and Tz8Si. The generality of the strong effect of polymer backbone mobility on proton conductivity is further illustrated by the data in Figure 4 for polyvinyltriazole (T_g = 48 °C, as measured in our lab) and polyvinylimidazole (T_g = 163 °C)[28] which follow the same general curve in spite of the large pK_a difference. The difference in glass transition temperature further supports our observations, indicating that addition of a third nitrogen to the heterocyclic motif has a profound effect in the nature of the resulting hydrogen-bonded network. This study suggests that the interactions between polymer matrix and heterocyclic motifs are more complex than originally anticipated and that they depend heavily on chemical structure. The difference between our results and those published by Zawodzinski and co-workers[19] may stem from the fact that their model compound study only considered systems where the heterocycle was not bound to a polymer matrix. Further exploration of these discrepancies will be necessary to fully understand their origin.

In order to study the effect of adding extra charge carriers on the proton conductivity of these systems, Tz2Si, Tz8Si, and FBz2Si were doped with varying amounts of trifluoroacetic acid (TFA) (see Figure 5). The acid doping produced conductivity increases of approximately 2 orders of magnitude throughout the studied temperature range. The optimal dopant concentration varied depending on the nature of the heterocycle. In the case of triazole-containing polysiloxanes Tz2Si and Tz8Si, the maximum conductivity increase was achieved at 75 mol % TFA, and addition of 100 mol % of TFA produced no further conductivity increases. The 2-trifluoromethylbenzimidazole-grafted polysiloxane, FBz2Si, reached the maximum value at 15 mol % TFA. The difference in behavior as a function of doping level is attributed to the third heteroatom in the triazole ring, which can be ionized without hindering the ability of the heterocycle to form dynamic hydrogen-bonded networks.

The observed conductivities for the doped polymers Tz8Si and FBz2Si constitute the highest conductivity values reported for anhydrously conducting polymers at temperatures below 100 °C (ranging from $10^{-3.5}$ to 10^{-5} S/cm), while above this temperature, the conductivity of Tz2Si is comparable, or superior, to that of the doped imidazole-containing analogs and other previous reports.[12,18,29−31]

In addition to high conductivity and chemical and thermal stability, any candidate material being considered for use a proton exchange membrane must also be electrochemically stable under fuel cell operation conditions. Cyclic voltammetry studies of the polysiloxanes Tz2Si, Tz8Si, and FBz2Si have shown no oxidative processes up to 2 V at 40 °C. The superior electrochemical stability of the 1,2,3-triazole ring over imidazole,[17,27] along with the ease of synthesis of the 1,2,3-triazole precursors via extremely efficient and chemoselective "click" procedures, makes extension of this approach particularly attractive.[32] Furthermore, the possibility of increasing the proton conductivity of the triazole-tethered polysiloxanes by addition of up to 1 mol equiv of acid could potentially allow their combination with strong acid containing materials to generate polymer blends or copolymers[33] able to transport protons under both humidified and anhydrous conditions.

Conclusions

The combination of flexible polymeric backbones and readily accessible, electrochemically stable, 1,2,3-triazoles produced materials exhibiting water-free proton conductivities higher than those previously reported at temperatures below 100 °C. The variations in the pK_a of the proton-conducting heterocycle did not influence the proton conductivity significantly, while the glass transition temperature of the polymer matrix and the mass fraction of the proton-conducting motifs proved the key dominating factors determining the proton conductivity of the polymer materials. The optimal composition to maximize proton conductivity depended significantly on the heterocycle's chemical structure. An extension of this work, using more complex polymer architectures and higher dielectric constant polymeric matrices, is currently underway and is expected to yield materials with proton conductivities suitable for membrane electrode assembly fabrication and testing.

Acknowledgment. Funding was provided by DOE EERE Subcontract #10759-001-05. Analytical facilities are made available through the NSF-supported Materials and Research Science and Engineering Center on Polymers at UMass Amherst (DMR-0213695). Mass spectral data were obtained at the University of Massachusetts Mass Spectrometry Facility which is supported, in part, by the National Science Foundation.

Supporting Information Available: ^{1}H NMR and ^{13}C NMR spectra and CV plots. This material is available free of charge via the Internet at http://pubs.acs.org.

References and Notes

(1) Parsons, I. *Fuel Cell Handbook*; EG & G Services, U.S. Department of Energy, O.o.F.F.E., 2000.
(2) Zalbowitz, M.; Thomas, S. *Fuel Cells: Green Power*; U.S. Department of Energy, 1999.
(3) Carrette, L.; Friedrich, K. A.; Stimming, U. *Fuel Cells* **2001**, *1*, 5−39.
(4) Steele, B. C. H.; Heinzel, A. *Nature (London)* **2001**, *414*, 345−352.
(5) Rikukawa, M.; Sanui, K. *Prog. Polym. Sci.* **2000**, *25*, 1463−1502.
(6) Rusanov, A. L.; Likhatchev, D. Y.; Mullen, K. *Russ. Chem. Rev.* **2002**, *71*, 761−774.
(7) Hickner, M. A.; Ghassemi, H.; Kim, Y. S.; Einsla, B. R.; McGrath, J. E. *Chem. Rev.* **2004**, *104*, 4587−4611.
(8) Li, Q.; He, R.; Jensen, J. O.; Bjerrum, N. J. *Chem. Mater.* **2003**, *15*, 2896−4915.
(9) Kreuer, K. D. *Solid State Ionics* **1997**, *94*, 55−62.
(10) Kreuer, K. D.; Fuchs, A.; Ise, M.; Spaeth, M.; Maier, J. *Electrochim. Acta* **1998**, *43*, 1281−1288.
(11) Schuster, M. E.; Meyer, W. H. *Annu. Rev. Mater. Res.* **2003**, *33*, 233−261.
(12) Herz, H. G.; Kreuer, K. D.; Maier, J.; Scharfenberger, G.; Schuster, M. F. H.; Meyer, W. H. *Electrochim. Acta* **2003**, *48*, 2165−2171.
(13) Schuster, M.; Rager, T.; Noda, A.; Kreuer, K. D.; Maier, J. *Fuel Cells* **2005**, *5*, 355−365.
(14) Schuster, M. F. H.; Meyer, W. H.; Schuster, M.; Kreuer, K. D. *Chem. Mater.* **2004**, *16*, 329−337.
(15) Goward, G. R.; Schuster, M. F. H.; Sebastiani, D.; Schnell, I.; Spiess, H. W. *J. Phys. Chem. B* **2002**, *106*, 9322−9334.
(16) Persson, J. C.; Jannasch, P. *Macromolecules* **2005**, *38*, 3283−3289.
(17) Zhou, Z.; Li, S. W.; Zhang, Y. L.; Liu, M. L.; Li, W. *J. Am. Chem. Soc.* **2005**, *127*, 10824−10825.
(18) Zhou, Z.; Liu, R.; Wang, J.; Li, S.; Liu, M.; Bredas, J. L. *J. Phys. Chem. A* **2006**, *110*, 2322−2324.
(19) Subbaraman, R.; Ghassemi, H.; Zawodzinski, T. A. *J. Am. Chem. Soc.* **2007**, *129*, 2238−2239.
(20) Woudenberg, R. C.; Yavuzcetin, O.; Tuominen, M.; Coughlin, E. B. *Solid State Ionics* **2007**, *178*, 1135−1141.
(21) Martwiset, S.; Woudenberg, R. C.; Granados-Focil, S.; Yavuzcetin, O.; Tuominen, M.; Coughlin, E. B. *Solid State Ionics*, in press (DOI: 10.1016/j.ssi.2007.07.005).
(22) Gilchrist, T. L. *Heterocyclic Chemistry*, 2nd ed.; John Wiley and Sons: New York, 1992.
(23) Belcher, R. *J. Chem. Soc.* **1954**, 4159.
(24) Loren, J. C.; Krasinski, A.; Fokin, V. V.; Sharpless, K. B. *Synlett* **2005**, 2847−2850.
(25) Thibault, R. J.; Takizawa, K.; Lowenheilm, P.; Helms, B.; Mynar, J. L.; Frechet, J. M. J.; Hawker, C. J. *J. Am. Chem. Soc.* **2006**, *128*, 12084−12085.
(26) Littke, A. F.; Schwarz, L.; Fu, G. C. *J. Am. Chem. Soc.* **2002**, *124*, 6343−6348.
(27) Scharfenberger, G.; Meyer, W. H.; Wegner, G.; Schuster, M.; Kreuer, K. D.; Maier, J. *Fuel Cells* **2006**, *6*, 237−250.
(28) Li, X.; Goh, S. H.; Lai, Y. H.; Wee, A. T. S. *Polymer* **2001**, *42*, 5463−5469.
(29) Persson, J. C.; Jannasch, P. *Chem. Mater.* **2006**, *18*, 3096−3102.
(30) Li, S.; Zhou, Z.; Liu, M.; Li, W.; Ukai, J.; Hase, K.; Nakanishi, M. *Electrochim. Acta* **2006**, 51, 1351−1358.
(31) Lee, S. Y.; Scharfenberger, G.; Meyer, W. H.; Wegner, G. *Adv. Mater.* **2005**, *17*, 626−630.
(32) Kolb, H. C.; Finn, M. G.; Sharpless, K. B. *Angew. Chem., Int. Ed.* **2001**, *40*, 2004−2021.
(33) Jeske, M.; Soltmann, C.; Ellenberg, C.; Wilhelm, M.; Koch, D.; Grathwohl, G. *Fuel Cells* **2007**, *7*, 40−46.

MA071715Q